



Soft Switching Boost Converter with an HI-Bridge Auxiliary Resonant Circuit

Anandhi.T.S¹, B. VamsiKrishna^{*2}

Assistant Professor, Dept. of ECE, Jerusalem College of Engineering, Chennai, Tamil Nadu, India¹

Assistant Professor, Dept. of ECE, Bharath University, Chennai, Tamil Nadu, India²

* Corresponding Author

Abstract: A soft-switching boost converter is presented in this paper. The conventional boost converter generates switching losses at turn ON and OFF, and this causes a reduction in the whole system's efficiency. The presented boost converter utilizes a soft switching method using an auxiliary circuit with a resonant inductor and capacitor, auxiliary switch, and diodes. Therefore, the presented soft-switching boost converter reduces switching losses more than the conventional hard-switching converter. In this paper, the performance of the proposed soft-switching boost converter is verified through the theoretical analysis, simulation, and experimental results.

KEYWORDS: Auxiliary resonant circuit, boost converter, soft-switching boost converter, zero-current switching (ZCS), zero-voltage switching (ZVS).

I. INTRODUCTION

SMPS have become smaller and lighter due to higher switching frequency. Hard Switching frequency causes lots of periodic losses at turn ON and turn OFF. This Resonant converters have been introduced to reduce the Switching losses[1][7][14].

To achieve the resonance many converters uses the auxiliary circuit which increases the complexity of the circuit as well as its cost[4][12].

For some resonant converters with an Auxiliary switch, the main switch enables Soft switching, while the auxiliary performs hard Switching[4][13]. These converters cannot improve the whole system's efficiency owing to the switching losses of the auxiliary Switch.

A new soft-switching boost converter with an auxiliary switch and resonant circuit is presented in this paper. The resonant circuit consists of a resonant inductor, two resonant capacitors, two diodes, and an auxiliary switch. The resonant capacitor is discharged before the main switch is turned ON and the current flows through the body diode. These resonant components make a partial resonant path for the main switch to perform soft switching under the zero-voltage condition using the resonant circuit. Compared with other soft-switching converters, the proposed converter improves the whole system's efficiency by reducing switching losses better than other converters at the same frequency [7]. In this paper, some simulation results are presented for a 100W, 1-kHz prototype boost converter using Metal Oxide Semiconductor Field Effect Transistor (MOSFET).

International Journal of Advanced Research in Electrical, Electronics and Instrumentation Engineering

(An ISO 3297: 2007 Certified Organization)

Vol. 4, Issue 9, September 2015

II. CONFIGURATION OF THE PROPOSED SOFT-SWITCHING BOOST CONVERTER

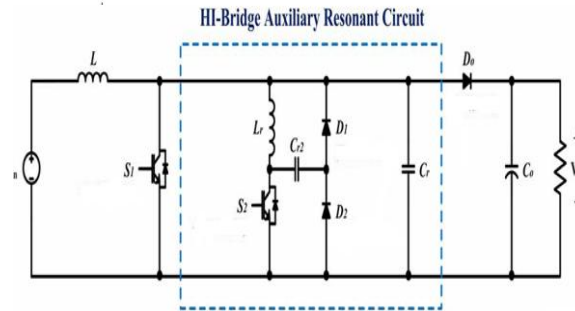


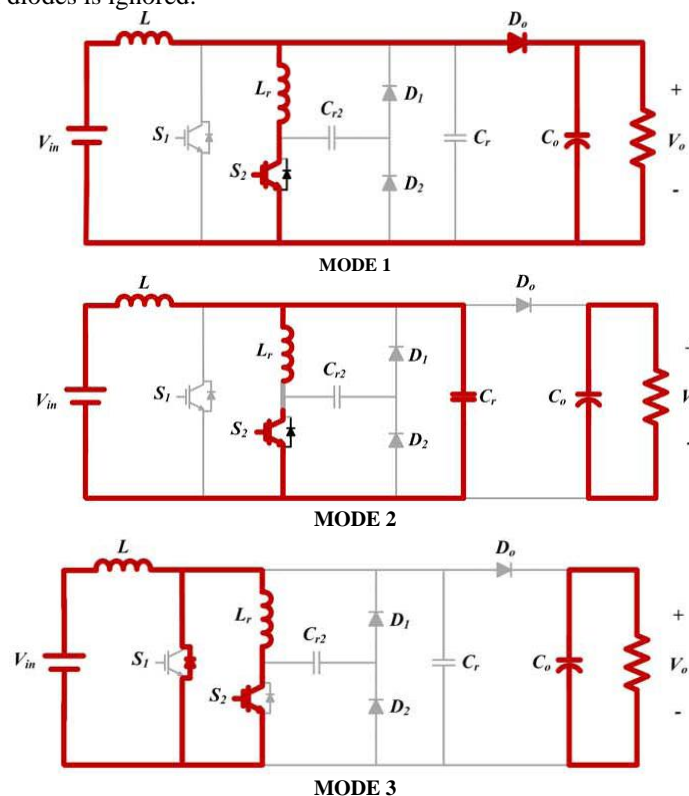
Figure 1 Shows the Circuit diagram of SSBC

The proposed converter is shown in Figure. 1. The main switch (S_1) and the auxiliary switch (S_2) of the proposed circuit enable soft switching through an auxiliary switching block, consisting of an auxiliary switch, two resonant capacitors (C_r and C_{r2}), a resonant inductor (L_r), and two diodes (D_1 and D_2).

III. OPERATIONAL ANALYSIS OF THE PROPOSED CONVERTER

The operational principle of the proposed converter can be divided into nine modes. For simple analysis of each mode of the proposed converter, the following assumptions are made

- 1) All switching devices and passive elements are ideal.
- 2) The input voltage (V_{in}) is constant.
- 3) The output voltage (V_o) is constant. (Output capacitor C_o is large enough.)
- 4) The recovery time of all diodes is ignored.



International Journal of Advanced Research in Electrical, Electronics and Instrumentation Engineering

(An ISO 3297: 2007 Certified Organization)

Vol. 4, Issue 9, September 2015

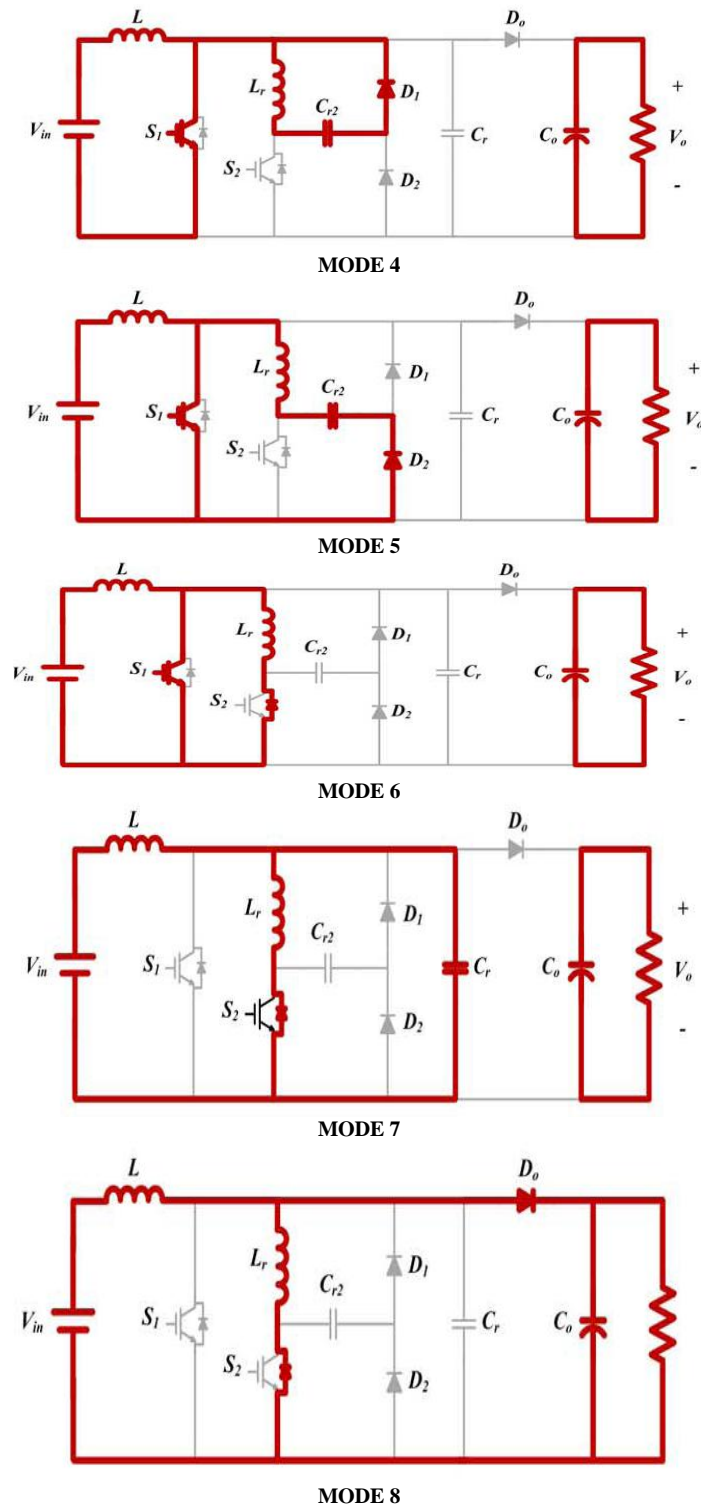


Figure 2 Operational modes of SSBC



International Journal of Advanced Research in Electrical, Electronics and Instrumentation Engineering

(An ISO 3297: 2007 Certified Organization)

Vol. 4, Issue 9, September 2015

Mode 1 operates in the range $t_0 < t < t_1$. When the auxiliary switch turns ON, mode 1 begins. After turning ON the auxiliary switch, the resonant inductor current begins to increase linearly from zero [2]. When the resonant inductor current (i_{Lr}) is equal to the main inductor current at t_1 , mode 1 completes and the resonant inductor voltage equals the output voltage. The main inductor current decreases and, at the end of this mode, the main inductor current is equal to zero [3].

Mode 2 operates in the range $t_1 < t < t_2$ immediately after the resonant inductor current and main inductor current have equalized, the main diode is turned OFF. The resonant capacitor Cr and the resonant inductor start their resonance, then the resonant capacitor Cr is discharged through resonant path Cr and Lr . After finishing the resonance, the resonant capacitor voltage is equal to zero. Mode 3 completes at t_2 [5]. At t_1 , the resonant inductor voltage is equal to the output voltage. The resonant inductor current is the sum of the main inductor and resonant current. The resonant capacitor Cr voltage is charged.

Mode 3 Operates in the range $t_2 < t < t_3$. The resonant capacitor (Cr) voltage has reached zero, the body diode of main switch is turned ON naturally. In this case, the main switch voltage is equal to zero and the turn-ON signal is given to the main switch under the zero-voltage condition. In this mode, the main inductor voltage is equal to the input voltage. After the resonance in mode 2, the resonant inductor current is constant. The resonant capacitor (Cr) voltage has been strongly discharged in mode 2. Therefore, the resonant capacitor voltage is zero.

Mode 4 Operates in the range $t_3 < t < t_4$. The main switch turns ON under the zero-voltage condition. When the auxiliary switch is turned OFF for the same condition, mode 4 begins. In this stage, the resonant inductor and resonant capacitor (Cr_2) start the resonance [6]. After the quarter-wave resonance of Lr and Cr_2 , the current of Lr is zero. Mode 4 is complete and Cr_2 has been fully charged by the resonance.

Mode 5 Operates in the range $t_4 < t < t_5$. After mode 4 completes, the current flow of the resonant inductor Lr reverses and the next stage starts. In mode 5, a reverse resonance of L and Cr_2 through the main switch and D_2 occurs. When the Cr_2 voltage has reached zero by resonance, the resonance of Lr and Cr_2 is complete and the Cr_2 voltage is zero. During modes 4 and 5, the resonant capacitor voltage is charged and discharged [8].

Mode 6 Operates in the range $t_5 < t < t_6$. After the Cr_2 voltage has reached zero, the body diode of the auxiliary switch is turned ON. The current flows through the freewheeling path of the body diode—the resonant inductor—the main switch. By the pulse width modulation (PWM) algorithm, when the main switch is turned OFF, this mode is complete. In this interval, the magnitude of the resonant inductor current is equal at t_2 . However, the current flow is reversed.

Mode 7 Operates in the range $t_6 < t < t_7$. When the main switch is turned OFF under the zero-voltage condition, mode 7 starts. The sum of the two inductor currents is the charging current of the resonant capacitor Cr in this mode. When the resonant capacitor (Cr) voltage is equal to the output voltage, this mode is completed. Because the two inductor currents charge the resonant capacitor Cr .

Mode 8 Operates in the range $t_7 < t < t_8$. At t_7 , the resonant capacitor Cr has been charged and the main diode voltage is zero. Therefore, the main diode turns ON under the zero-voltage condition and the resonant inductor current decreases linearly toward zero. After the current has reached zero, mode 8 completes and the next switching cycle starts.

IV. DESIGN AND IMPLEMENTATION OF COMPONENTS

The duty ratio is calculated using equation (1)

$$D = 1 - \frac{V_{i_{ms}}}{V_o} \quad (1)$$



International Journal of Advanced Research in Electrical, Electronics and Instrumentation Engineering

(An ISO 3297: 2007 Certified Organization)

Vol. 4, Issue 9, September 2015

Critical inductance is calculated from equation (2)

$$L_c = L = \frac{(1-D)DR}{2f} \quad (2)$$

Critical capacitance is calculated from equation (3)

$$C_c = C = \frac{D}{2RF} \quad (3)$$

Resonant inductance is calculated from equation (4)

$$L_r = \frac{V_0}{i_{L_r}(t)} t \quad (4)$$

Where $i_{L_r}(t) = i_{min}$

Resonant capacitance is calculated from equation (5)

$$C_r < \frac{D_{min}^2}{\pi^2 L_r f_s^2} + \frac{i_{min}^2 L_r}{\pi^2 V_0^2} \quad (5)$$

The time consisted of the resonant time between L_r and C_r , and the time that the resonant inductor current takes to become equal to the input current. After the delay time, the energy has accumulated in the main inductor. The switch is turned ON like a conventional boost converter [11]. Thus, when the auxiliary switch is turned ON, the effect on the total duty is larger [9].

The converter is designed based on the above equations.

Parameters of the presented soft switching boost converter are shown in the below table I.

TABLE I SIMULATION PARAMETERS

Parameters	Symbol	Value	Unit
Input voltage	Vin	12	V
Output voltage	Vo	48	V
Main inductor	L	3.85	μH
Resonant inductor	Lr	4.26	μH
Resonant capacitor	Cr	20	nF
Auxiliary capacitor	Cr ₂	10	nF
Output Capacitor	Co	1000	μF
Switching Frequency	f _{sw}	1	KHz

International Journal of Advanced Research in Electrical, Electronics and Instrumentation Engineering

(An ISO 3297: 2007 Certified Organization)

Vol. 4, Issue 9, September 2015

V. SIMULATION RESULTS

The MATLAB Simulation software is used to analyze the boost converter and soft switching boost converter with an HI-Bridge Auxiliary resonant circuit [10]. These are designed using the parameters given in the table I. The simulink is the tool for modeling, simulating, analyzing multi domain dynamic systems.

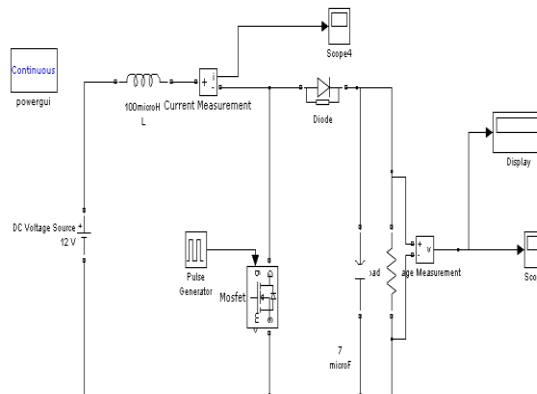


Figure 3 Simulink diagram of Boost Converter

Figure 3 shows the simulink diagram of the conventional boost converter which has a main switch, main inductor, capacitor. The output voltage 48V is obtained across the load resistor.

Figure 4 shows the switch current, voltage, inductor current and gate pulse waveform respectively of conventional boost converter respectively [15]. When the switch is turned on the inductor current increases linearly from zero, the switch current increases and the switch voltage decreases, but during the turn on of the switch of the conventional boost converter both the switch voltage and switch current are present leading to switching losses [17-19].

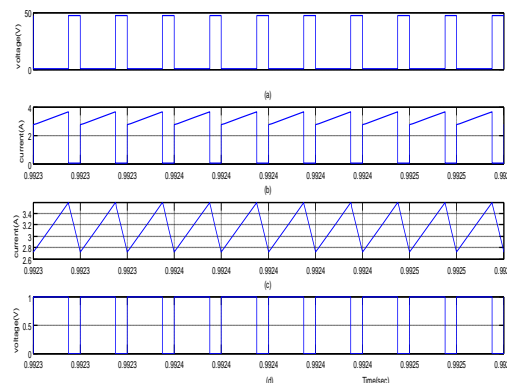


Figure 4 (a) Main switch voltage (b) main switch current (c) inductor current (d) switching waveform

International Journal of Advanced Research in Electrical, Electronics and Instrumentation Engineering

(An ISO 3297: 2007 Certified Organization)

Vol. 4, Issue 9, September 2015

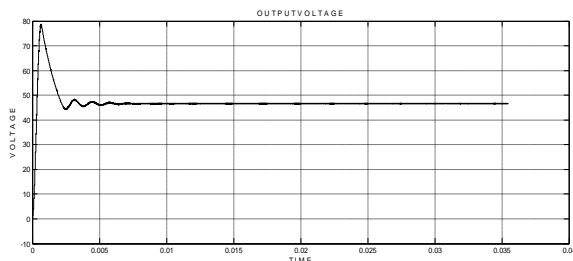


Figure 5 Output Waveform of Boost Converter

Figure 5 shows the output waveform of the boost converter.

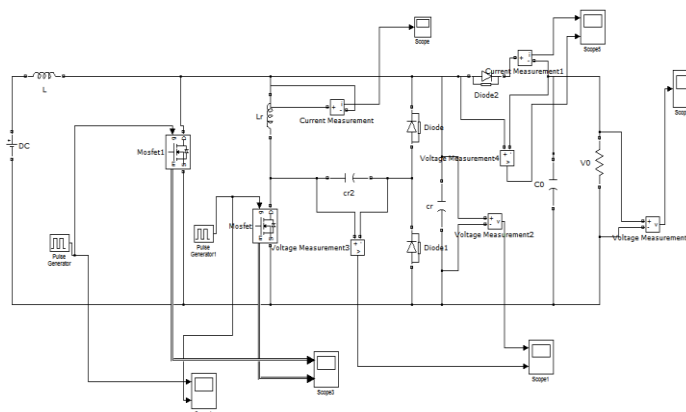


Figure 6 Simulink Diagram of SSBC

Figure 6 shows open loop diagram of SSBC. For above circuit component values are designed and simulated using MATLAB package. For an input voltage of 12V, desired output voltage 48V was obtained.

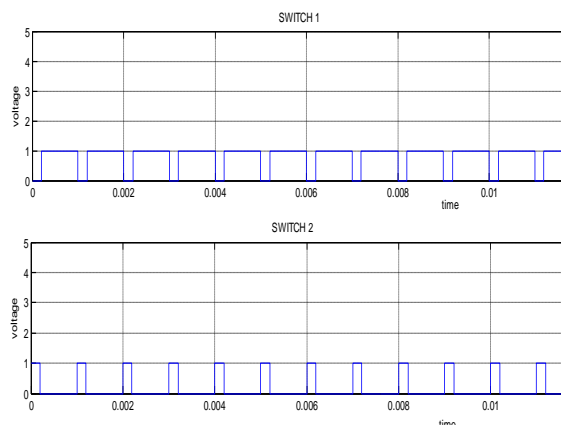


Figure 7 Switching Waveform of SSBC for Open loop

Figure 7 shows switching wave form of SSBC. According to the modes of operation first auxiliary switch turned ON. When the auxiliary switch turned OFF at that instant Main switch turned ON, this will be shown in above figure. Figure 8 shows Resonant inductor current which increases linearly from Zero, when the auxiliary switch turned ON and also the switching waveform of the main switch and auxiliary switch are shown.

International Journal of Advanced Research in Electrical, Electronics and Instrumentation Engineering

(An ISO 3297: 2007 Certified Organization)

Vol. 4, Issue 9, September 2015

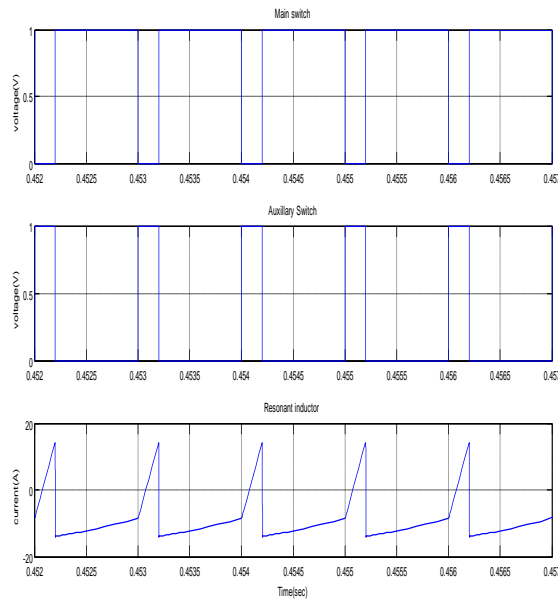


Figure 8 Switching waveform and Resonant inductor current

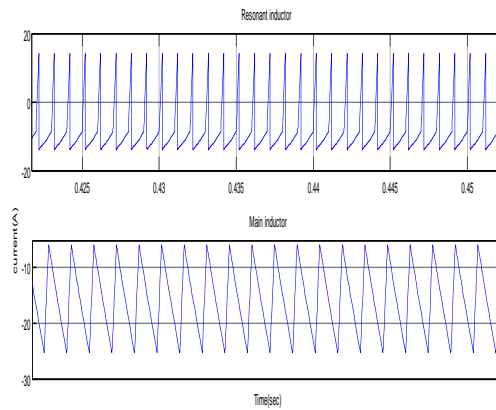


Figure 9 Resonant inductor and Main Inductor current

Figure 9 shows the resonant inductor current and main inductor current waveform. According to the operating mode when both inductor current will equal then resonant inductor voltage equal to the output voltage [16].

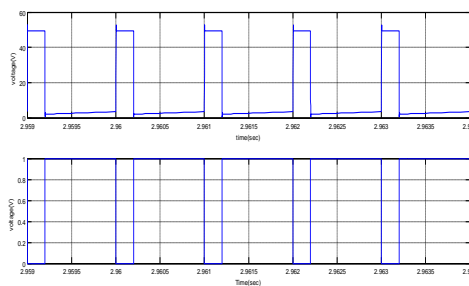


Figure 10 Resonant Capacitor voltage and main switch Waveform

International Journal of Advanced Research in Electrical, Electronics and Instrumentation Engineering

(An ISO 3297: 2007 Certified Organization)

Vol. 4, Issue 9, September 2015

Figure 10 shows the resonant capacitor voltage waveform. The main Switch will turn ON when the resonant capacitor voltage has reached zero.

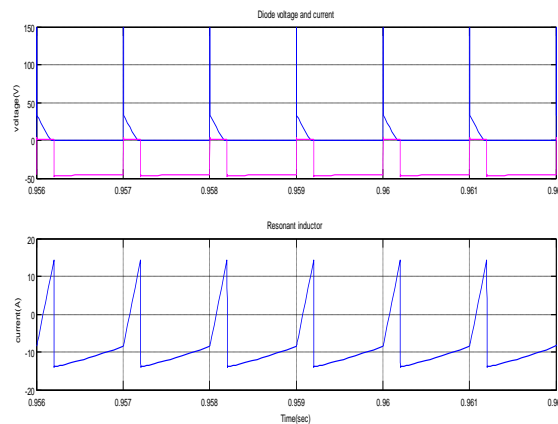


Figure 11 Diode waveforms and Resonant inductor

Figure 11 shows the voltage and current waveform of the main diode. The waveform shows that the diode is turned on under ZVS condition as the inductor current is zero at the point of turn on of the diode.

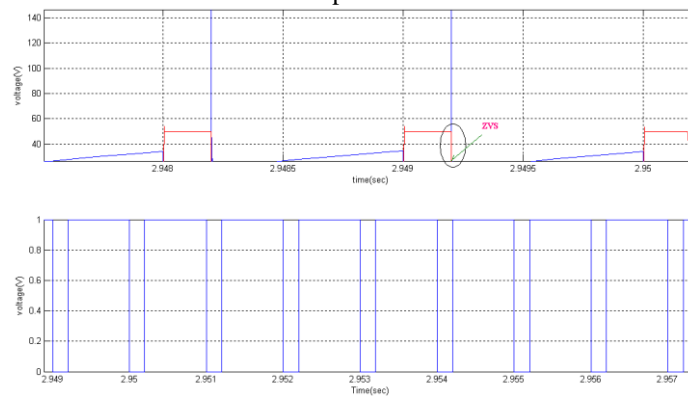


Figure 12 Zero Voltage Switching Condition in Main Switch

Figure 12 shows the ZVS condition in main switch. The main switch turns ON under the zero-voltage condition. When the main switch voltage reaches zero

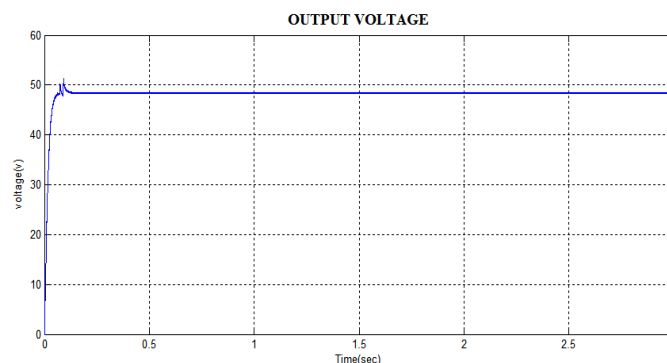


Figure 13 Output Waveform of Open Circuit for SSBC



International Journal of Advanced Research in Electrical, Electronics and Instrumentation Engineering

(An ISO 3297: 2007 Certified Organization)

Vol. 4, Issue 9, September 2015

Figure13 shows the output voltage waveform of the soft switching boost converter. The output is taken from the load resistor.

VI. CONCLUSION

For chosen parameters the expected output voltage using soft switching boost converter is designed and developed. The output voltage and inductor current obtained is greater than the expected level. The soft switching boost converter minimizes the output voltage ripple and input current ripple. Hence the Soft Switching Boost Converter achieves ZVS. The operation principles and theoretical analysis of the proposed converter have been confirmed by simulation and a prototype of 100 W and 1 kHz. The proposed converter is suitable for applications such as high-efficiency converters, photovoltaic dc/dc converters, a power-factor-correction circuit, and battery chargers.

REFERENCES

1. G. Hua , C.S. Leu, Y. Jiang, and F. C. Y. Lee, "Novel-voltage transition PWM converters," *IEEE Trans.Power Electron.*, vol. 9, no. 2,pp. 213–219, Mar. 1994
2. Babu T.A., Sharmila V., "Cefotaxime-induced near-fatal anaphylaxis in a neonate: A case report and review of literature", *Indian Journal of Pharmacology*, ISSN : 0253-7613, 43(5) (2011) pp.611-612.
3. G. Hua, E. X. Yang, Y. Jiang, and F. C. Y. Lee, "Novel zero-current transition PWM converters," *IEEE Trans Power Electron.*, vol. 9, no. 6,pp. 601–606, Nov. 1994.
4. H. Bodur and A. F. Bakan, "A new ZVT-ZCT-PWM DC-DC converter,"*IEEE Trans. Power Electron.*, vol. 19, no. 3, pp. 676–684, May 2004.
5. H. Bodur and A. F. Bakan, "A new ZVT-PWM DC-DC converter," *IEEE Trans. Power Electron.*, vol. 17, no. 1, pp. 40–47, Jan. 2002.
6. Valiathan G.M., Thenumgal S.J., Jayaraman B., Palaniyadi A., Ramkumar H., Jayakumar K., Bhaskaran S., Ramanathan A., "Common docking domain mutation e322k of the erk2 gene is infrequent in oral squamous cell carcinomas", *Asian Pacific Journal of Cancer Prevention*, ISSN : 1513-7368, 13(12) (2012) pp.6155-6157.
7. S. S. Saha, B. Majumdar, T. Halder, and S. K. Biswas, "New fully softswitched boost-converter with reduced conduction losses," in *Proc. Power Electron. Drive Syst. 2005 Int. Conf.*, Jan., 2006, vol. 1, pp. 107–112.
8. N. Jain, P. K. Jain, and G. Joos, "A zero voltage transition boost converter employing a soft switching auxiliary circuit with reduced conduction losses," *IEEE Trans. Power Electron.*, vol. 19, no. 1, pp. 130–139, Jan. 2004.
9. Mani Sundar N., Krishnan V., Krishnaraj S., Hemalatha V.T., Alam M.N., 'Comparison of the salivary and the serum nitric oxide levels in chronic and aggressive periodontitis: A biochemical study', *Journal of Clinical and Diagnostic Research*, ISSN : ISSN - 0973 - 709X, 7(6) (2013) pp.1223-1227.
10. B. R. Lin and J. J. Chen, "Analysis and implementation of a soft switching converter with high-voltage conversion ratio," *IET Power Electron.*, vol. 1, no. 3, pp. 386–394, Sep. 2008.
11. L. Jong-Jae, K. Jung-Min, K. Eung-Ho, and K. Bong-
12. Hwan, "Dual series resonant active clamp converter," *IEEE Trans Ind. Electron.*, vol. 55, no. 2, pp. 699–710, Feb. 2008.
13. X. Wu, J. Zhang, X. Ye, and Z. Qian, "Analysis and derivations for a family ZVS converter based on a new active clamp ZVS cell," *IEEE Trans. Ind. Electron.*, vol. 55, no. 2, pp. 773–781, Feb. 2008.
14. D. W. Erming and A. R. Hefner, Jr., "IGBT model validation for soft switching applications," *IEEE Trans Ind. Appl.*, vol. 37, no. 2, pp. 650–660, Mar./Apr. 2001.
15. S.-R. Park, S.-H. Park, C.-Y. Won, and Y.-C. Jung, "Low loss soft switching boost converter," in *Proc. 13th Power Electron. Motion Control Conf.* 2008, Sep. 2008, pp. 181–186.
16. Thirunavukkarasu A.B., Chandrasekaran V., 'Efficacy of anti-scorpion venom serum over prazosin in severe scorpion envenomation: Is the current evidence enough', *Journal of Postgraduate Medicine*, ISSN : 0022-3859, 57(1) (2011) pp.83-84
17. H. Mao, O. A. Rahman, and I. Batarseh, "Zero-voltage-switching DC-DC converters with synchronous rectifiers," *IEEE Trans. Power Electron.*, vol. 23, no. 1, pp. 369–378, Jan. 2008.
18. P. Das, B. Laan, S. A. Mousavi, and G. Moschopoulos, "A Non isolated bidirectional ZVS-PWM active clamped DC-DC converter," *IEEE Trans. Power Electron.*, vol. 24, no. 2, pp. 553–558, Feb. 2009.
19. Subbaraj G.K., Kulanthaivel L., Rajendran R., Veerabathiran R., "Ethanol extract of *Carum carvi* (EECC) prevents N-nitrosodiethylamine induced phenobarbital promoted hepatocarcinogenesis by modulating antioxidant enzymes", *International Journal of Pharmacy and Pharmaceutical Sciences*, ISSN : 0975 - 1491, 5(S1) (2013) pp.195-199.
20. J.-H. Kim, D.-Y. Jung, S.-H. Park, C.-Y. Won, Y.-C. Jung, and S.-W. Lee, "High efficiency soft-switching boost converter using a single switch," *J. Power Electron.*, vol. 9, no. 6, pp. 929–939, Nov. 2009.
21. B Karthik, S Rajeswari, Design and Analysis of a Transceiver on a Chip for Novel IR-UWB Pulses, *Middle-East Journal of Scientific Research* 19 (6), PP 817-820, 2014.
22. Shriram, Revati; Sundhararajan, M; Daimiwal, Nivedita; , Application of High & Low Brightness LEDs to Human Tissue to Capture Photoplethysmogram at a Finger Tip Red, V-620, PP 700.
23. Muralibabu, K; Sundhararajan, M; , PAPR performance improvement in OFDM system using DCT based on adjacent symbol grouping *Trans Tech Publ, Applied Mechanics and Materials*, V-550, PP 204-209, 2014.
24. sivaperumal, s; sundhararajan, m; , advance feature extraction of mri brain image and detection using local segmentation method with watershed.
25. MURALIBABU, K; SUNDHARARAJAN, M; , PAPR reduction using DCT based sub carrier grouping with Companding Technique in OFDM system.
26. Kanniga, E; Srikanth, SMK; Sundhararajan, M; , Optimization Solution of Equal Dimension Boxes in Container Loading Problem using a Permutation Block Algorithm *Indian Journal of Science and Technology*, V-7, I-S5, PP 22-26, 2014